From Partial Element Equivalent Circuit (PEEC) to muphyPEEC for Solving Coupled Multiphysics Problems

Vjosa Shatri[1], Ruzhdi Sefa[2], Lavdim Kurtaj[3], and Avni Skeja[4]

[1] **Department of Fundamental Engineering Subjects, Faculty of Electrical and Computer Engineering, University of Prishtina Prishtina, 10000, Kosovo**

[2] **Department of Fundamental Engineering Subjects, Faculty of Electrical and Computer Engineering, University of Prishtina Prishtina, 10000, Kosovo**

[3] **Department of Automation, Faculty of Electrical and Computer Engineering, University of Prishtina Prishtina, 10000, Kosovo**

[4] **Department of Automation, Faculty of Electrical and Computer Engineering, University of Prishtina Prishtina, 10000, Kosovo**

Abstract

A tool for unified simultaneous simulation of multiphysics problems based on Partial Element Equivalent Circuit (PEEC) method is presented. Extension of PEEC method with thermal and mechanical domains is based on circuit interpretation of Finite Difference (FD) and Finite Element Method (FEM) equations. Equations in FEM case are derived by Galerkin's residual method with basis functions of order zero or one. All steps of the process, from geometry description to netlist generation, are done with multiphysics PEEC (muphyPEEC) Toolbox for MATLAB. Solution of the problem is done with LTspice, where time- and frequency-domain simulations can be done. To demonstrate the approach, muphyPEEC is used to model and solve cooling of TO220 transistor mounted on flat plate heat sink and fin heat sink, and results are compared with IR (Infra Red) camera recordings. Electro-thermal microactuator is used as fully coupled problem example, and results are compared with those published elsewhere.

Keywords: *Partial Element Equivalent Circuit, PEEC, PEEC MATLAB Toolbox, Multiphysics PEEC, muphyPEEC, Flat Plate Heat Sink, Fin Heat Sink, Electro-Thermal Microactuator.*

1. Introduction

Equivalent circuits are widely used in electrical engineering community as very efficient tool for analyzing and simulating problems of different physical nature. One tries to describe problem with components common to electric/electronic circuits [1], and to use typical circuit analysis and simulation tools, like members of SPICE (Simulation Program with Integrated Circuit Emphasis) family [2], [3], [4], [5], [6], [7], for obtaining results. Development of equivalent circuit requires deep knowledge of problem and expressing its behavior with a set of equations, algebraic, differential, or partial differential. After some approximations and based on similarities with equations for electric circuits, analogies are developed [8], [9], [10], where electric circuit components will represent components from other physical domains, while electric variables, currents and voltages, will represent variables of other physical domains. Request for reliable circuit behavior prediction, at ever increasing operation frequency range, extends beyond classical "circuit of electrical and electronic components" as sufficient description, and extension with geometry of connections itself [11], even with components construction geometry details, is becoming a must. Partial Element Equivalent Circuit (PEEC) [12], [13] method can handle these combined electromagnetic-circuit problems by developing equivalent circuit from geometry description, and combining them with other electric and electronic circuit components [14], [15], [16]. Circuit components and sources are sites for couplings with other physical domains, like thermal and mechanical. In single domain analysis circuit components are considered constant, and are calculated for some given operation point. If variability of components or of sources is highly dependent from physical variables, then it will be necessary to account this dependence during simulation. Influencing variables may be from the same physical domain, from other physical domains, and in general more than one physical domain may influence same circuit component. Since most solvers are designed and specialized for single domain, first approach is to use these solvers in their own field of expertise and create interface for exchanging results between them [17], [18]. Using results from other domains, each domain will recalculate component values for the new operation point. This process is iterated until steady state condition is reached in all physical domains for given time step. Other approach is unification of all physical domain

Copyright (c) 2013 International Journal of Computer Science Issues. All Rights Reserved.

equations and solving them simultaneously. PEEC method has been selected as unification platform for solving coupled multiphysics problems. General approach is in developing partial element circuits for discretized structures for each physical domain and corresponding couplings between them. Equivalent circuit is obtained by circuit interpretation of equations obtained by finite difference (FD) or finite element methods (FEM). In FEM case Galerkin's residual method with basis functions of order zero or one is used, the one (with basis functions of order zero) used also for developing electromagnetic PEEC.

2. Adding other Physical Domains to the PEEC Method

PEEC method for electromagnetic problems [12], [13], defines the building block equivalent circuits for discretized current (volume) and potential (surface) cell. Whole model is created by connecting all building blocks for all cells present in a discretized structure. Current cell is represented with series connection of one resistor and one inductor connected between two neighboring nodes of discretized structure in each dimension direction. For one-dimensional discretization (1D) cells are generated only in length direction. Two-dimensional discretizations (2D) have cells in two directions, usually one is length direction and other direction may be width or height. Three-dimensional discretizations (3D) have cells in all three directions, length, width, and height. Potential cell is modeled with single capacitor from node to the ground (infinity). As standard part are inductive and capacitive couplings. Extension of PEEC method to other physical domains is done by defining multiphysics PEEC building block. This multiphysics block will have a number of single domain blocks, at least one for every domain of interest, and corresponding couplings. For given problem not necessarily all cells will include building blocks from all domains, and all possible couplings. If one physical domain interacts with other domain over limited space, with some approximations problems can be decoupled, leading to system level simulations with FEM (possibly single domain) applied only inside some blocks, while for others higher level or lumped description can be used. If discretization for different domains is done with different mesh sizes, multiphysics cell may contain one single domain block for coarsest discretized domain but may have many single domain blocks for finer discretized domains.

3. Electromagnetic-Thermal PEEC Model

Balance equation as a partial differential equation that governs unsteady state heat transfer problem [19] in solids is

$$div(\kappa\, grad\, T) + G = c_V \frac{\partial T}{\partial t} \qquad \text{in } V, \tag{1}$$

or in cartesian coordinates [34]

$$\frac{\partial}{\partial x}\left(\kappa \frac{\partial T}{\partial x}\right) + \frac{\partial}{\partial y}\left(\kappa \frac{\partial T}{\partial y}\right) + \frac{\partial}{\partial x}\left(\kappa \frac{\partial T}{\partial y}\right) + G = c_V \frac{\partial T}{\partial t}, \tag{2}$$

with boundary conditions at each point of the surface S [20], [21] as a given temperature T_b (Dirichlet boundary condition) on S_T part of the surface

$$T = T_b \qquad \text{on } S_T, \tag{3}$$

a given flux Q_b (Neumann boundary condition) on S_Q part of the surface

$$-\kappa \frac{\partial T}{\partial n} = Q_b \qquad \text{on } S_Q, \tag{4}$$

or convection condition with the environment (Robin boundary condition) on S_C part of the surface

$$-\kappa \frac{\partial T}{\partial n} = h(T - T_e) \qquad \text{on } S_C, \tag{5}$$

where n is outward normal vector to the boundary, and T_e is environment temperature. Material properties are represented by volumetric heat capacity c_V, and by thermal conductivity coefficient κ. G represents all body sources of heat, with possibility of being dependent on space and time. Equations are solved for unknown temperature field T.

Two classical methods for solving problem numerically are finite difference method (FDM) and finite element method (FEM). Both methods require discretization of three dimensional structures to a number of cells. FDM uses finite differences to approximate derivatives of balance and boundary conditions equations [22], [23], [24], [25]. For circuit interpretation only space derivatives are approximated with finite differences, while time derivatives are part of constructed equivalent circuit. Equivalent circuit for single discrete element (cell) is composed from one capacitance (thermal capacity), between node in the cell center and ground, and with resistors (thermal resistors), from this center node to each volume face [26], [27], [28]. FEM approach for solving

Copyright (c) 2013 International Journal of Computer Science Issues. All Rights Reserved.

thermal problem usually uses some of weighted residual method, with Galerkin's residual method being particularly popular [29], [20], [19], and will result with semi-discrete matrix equation of form [30], [19], [31]

$$\boldsymbol{C}\frac{\partial \boldsymbol{T}(t)}{\partial t}+\boldsymbol{K}\boldsymbol{T}(t)=\boldsymbol{G}(t), \qquad (6)$$

where matrix $\boldsymbol{C}$ is a symmetric thermal capacitance matrix, $\boldsymbol{K}$ is a symmetric thermal conductivity matrix, $\boldsymbol{G}$ is the thermal load vector [31], and $\boldsymbol{T}(t)$ is vector of nodal temperatures. Circuit interpretation comes directly by comparing them with modified nodal analysis equations [5], [4]. Matrix **C** can be interpreted as a circuit by self- and mutual-capacitors, C_{ii} and C_{ij}, [30], [32], matrix $\boldsymbol{K}$ by resistors between corresponding nodes [30], and vector $\boldsymbol{G}$ with current or voltage sources (ideal and real) [30]. In general case $\boldsymbol{C}$ matrix generated by FEM method is block-diagonal, but often diagonal, or lumped, form is used [33], [19], although it is not unconditionally stable.

Electromagnetic PEEC method is derived by using constant basis functions (0th-order or pulse functions) for developing unknown fields over discretized structure, and as Galerkin weighting functions [12], [13], with procedures similar to FEM, with final circuit interpretation of space-discretized equations. FEM thermal model follows similar pathway. Structure discretization for one domain, in general, can be different from discretization for other one. Discretization for electromagnetic domain is twofold, into volume current cells and surface potential cells. Volume cells for each dimension lies between two neighboring nodes of same dimension, whereas one potential cell is attached to each surface node. Discretization for thermal domain will have one volume cell per each volume node, with node being in the center of adopted trial basis function. Relation between these two discretizations will lead to different number of cells and computational requirements during simulation. Fig. 1 shows four possible arrangements for 2-dimensional (2D) discretization. In Fig. 1(a) nodes of two discretizations overlap, with total of (s+1)·(w+1) thermal cells, where s and w is number of current cells in length and width direction. In this configuration four electrical resistors contribute to heat generation inside single cell, each with half of its dissipated power. Nodes on edges and on corners have three and two electrical resistors, correspondingly, that contribute to heat generation. For clarity current cells are made thinner in one from two dimensions, and with normal size spanning to midway between nodes.

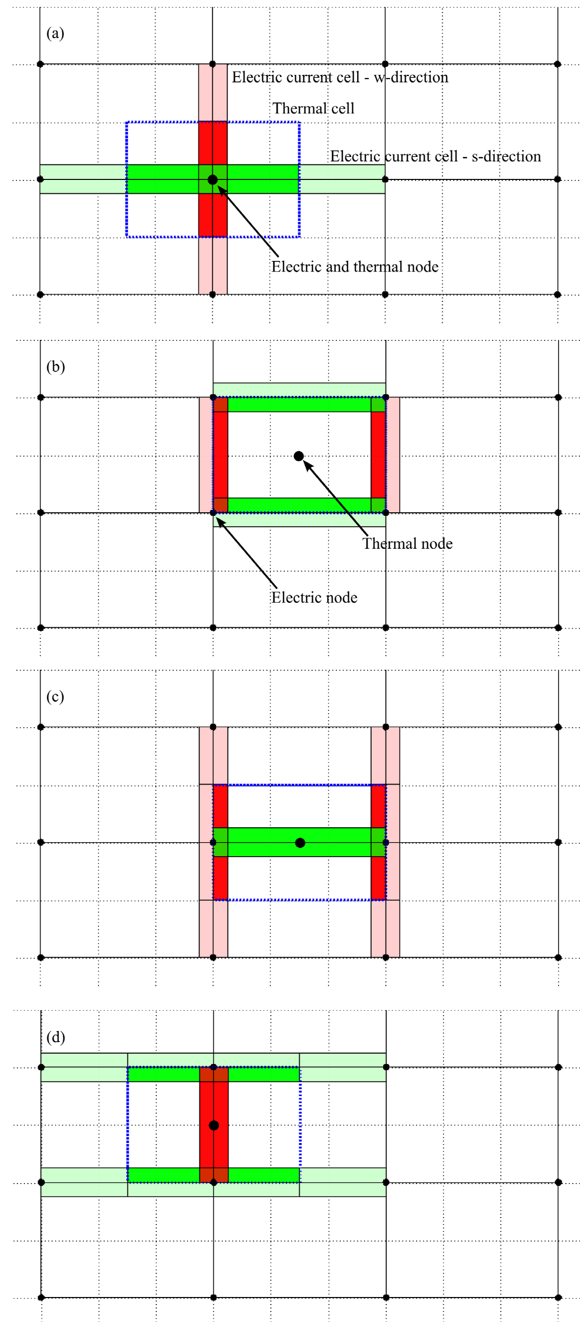

Fig. 1 Arrangements between 2D electrical and thermal discretizations: (a) Overlapped nodes, (b) Thermal cell between four electrical nodes, (c) Thermal cell coincides with electrical current cell in length direction, (d) Thermal cell coincides with electrical current cell in width direction. Electric current cells are made thinner in one from two dimensions for clearer view. Green current cells are in length direction (s), and red current cells are in width direction (w). Parts of current cells (resistors) that contribute to heat generation for given thermal cell (dashed blue line) are highlighted.

Part of resistor that contributes to heat generation inside cell is highlighted. Configuration in Fig. 1(b) has thermal cells situated between for electrical nodes, with total of s·w

Copyright (c) 2013 International Journal of Computer Science Issues. All Rights Reserved.

thermal cells. Thermal node is in middle of thermal cell. This configuration is typical for FDM. Two other cases from Fig. 1, (c) and (d), have preferred direction for thermal cell alignment, in length or width direction of electrical current cells. Last two cases for 1D discretization would have one-to-one correspondence between electrical current cell and thermal cell. Similar configurations can be developed for 3D discretization. Fig. 2 shows only case with overlapped nodes with (s+1)·(w+1)·(h+1) thermal cells, h is number of current cells in height direction. Six electrical resistors will contribute to heat generation inside internal cell. Electromagnetic PEEC cell and equivalent circuits for thermal model can be combined by taking into account couplings that may exist between two domains to create electromagnetic-thermal PEEC model. Couplings in this case include only direct influences of one domain to the other. Fist influence is from electric domain to the thermal one by heat generated from resistive power losses, and will be distributed over volume where current flows. It will be modeled as heat generating current source in thermal equivalent circuit, dependent from power losses in all resistors (or parts of resistors) inside thermal cell. In spice like simulators it will be a B-source type, i.e. arbitrary behavioral current source [4], [6], [7]. Second direct influence is from thermal domain to electric one through temperature dependent electric circuit components. Since temperature is modeled with voltage, they would be voltage dependent resistors [6], [35], voltage dependent capacitors [27], [35], [36], and voltage dependent inductors [6], [35], [36].

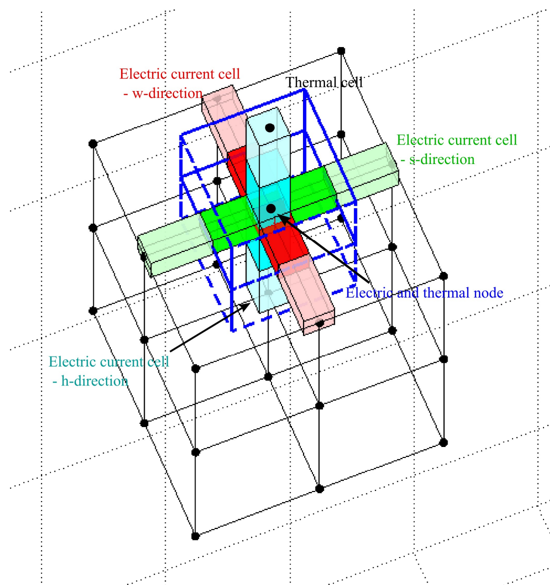

Fig. 2 Arrangements between 3D electrical and thermal discretizations with overlapped nodes. Electric current cells are made thinner in two from three dimensions for clearer view.

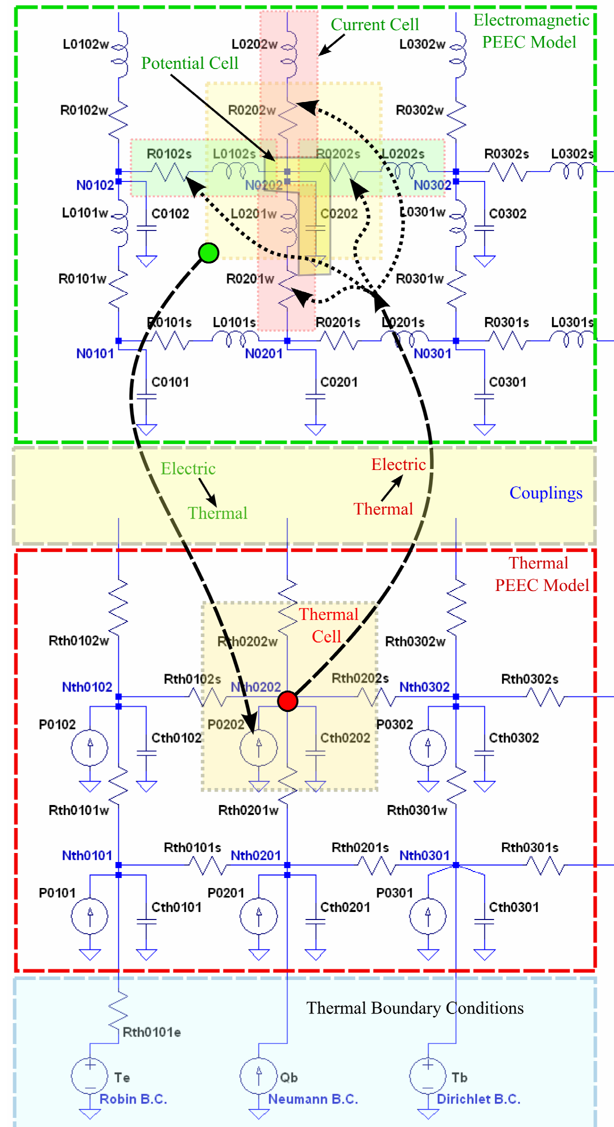

Fig. 3 2D PEEC model for part of a conductor cells with coupled electromagnetic-thermal interactions.

In the strict sense, indirect influences mediated by other domains, ex. thermally induced mechanical deformations, are not included here. 2D PEEC model for part of a conductor cells with coupled electromagnetic-thermal interactions is given in Fig. 3. Capacitive and inductive couplings present in standard electromagnetic PEEC model [12], [13], [15], are not shown in this figure. Part of thermal PEEC model corresponds to FEM type with 0th order basis functions, and is similar to FDM with difference only in peripheral cells circuit model [26]. Three types of boundary conditions are shown at the bottom of Fig. 3. Any boundary condition can be applied to any peripheral node. Parts of the thermal model without

Copyright (c) 2013 International Journal of Computer Science Issues. All Rights Reserved.

internal heat generation inside corresponding thermal cells will miss current sources

Depending on the problem to be analyzed, model can be made simpler by removing circuit components, electric or thermal, and influences. Ex. for magneto-quasi-static and stationary currents problems simplified [R, L] electric model can be used [13], [15], where capacitors, capacitive couplings, and retardation is ignored. Or, if only steady-state temperature field is of interest, thermal capacities can be ignored. For problems with very low electric power losses, influence of electric domain to thermal domain can be ignored, but temperature influence on electric domain will be accounted for. In other cases temperature dependence of electric components can be ignored, but heating from electric power losses will be modeled.

4. Mechanical PEEC Model

By applying FEM to partial differential equations which describes the behavior of elastic body, a second order matrix differential equations is obtained [21]

$$\boldsymbol{M}\ddot{\boldsymbol{x}}(\boldsymbol{t}) + \boldsymbol{C}\dot{\boldsymbol{x}}(\boldsymbol{t}) + \boldsymbol{K}\boldsymbol{x}(\boldsymbol{t}) = \boldsymbol{B}\boldsymbol{u}(\boldsymbol{t}), \quad (7)$$

where M is mass matrix, C is damping matrix, and K is stiffness matrix. $Bu(t)$ is the load vector and $x(t)$ is unknown vector to be found with a number of degrees of freedom. If $x(t)$ is made analogous to electric charge $q(t)$, M matrix will be implemented with inductors, C matrix with resistors, and K matrix will be implemented with capacitors [8], [10]. Load vector will be implemented with voltage generators.

5. muphyPEEC Toolbox

To solve coupled multi-domain (multiphysics) problems with PEEC method, MATLAB PEEC toolbox [16], [15], has been extended with functions for handling additional domains, and **mul**ti**phy**sics **P**artial **E**lement **E**quivalent **C**ircuit toolbox for MATLAB is created (**muphyPEEC**). Flow-diagram is similar to one described in [16], but steps for meshing, partial elements calculation, and LTspice netlist generation (for other domains Multisim compatible netlist generation is not supported any more) are done for all requested domains (electromagnetic, thermal, and mechanical). Meshing can be of different resolution for all domains, controlled globally or element-wise. Domain affiliation can also be controlled globally or element-wise. Separate netlist file is generated for each domain. They all have to be included in LTspice, where lumped circuit components are added, boundary conditions are set to required test conditions, and specific vales are given to parametric quantities, like material thermal conductivity, or material elasticity. Any experiment with new conditions in LTspice environment doesn't need regeneration of netlist files. If specific conditions are nedeed, even direct editing of netlist files can be done. Node and partial element naming makes this process easier, and less likely prone to errors. Calculation of partial elements for other domains is done locally without calling any external application, like was done for electromagnetic domain when FastCap2 and FastHenry2 were called. Calculation of view factors for radiative heat transfer is not covered yet, but if values for them are known they can be included in simulation as radiative boundary condition.

6 Simulation Examples

To demonstrate applicability of multiphysics PEEC to solve problems with coupled physical domains three examples has been selected and solved. In some cases results were compared with recordings with infra-red (IR) camera, in other results were compared with those published elsewhere. All circuit simulations were done in LTspice.

6.1 Flat plate heat sink with asymmetrically mounted transistor in TO220 case

Cooling high-power semiconductor devices is necessity for keeping device junction below maximum allowable working temperature. Heat sinks are used for dissipating into surrounding medium. Flat plate heat sinks are used for cooling lower range of power devices, and often using already existing metallic plates, ex. equipment cases. This example is about cooling transistor BDX53C in TO220 case. Cooler is flat Aluminium plate with dimensions 115mm in length, 35mm wide, and 3mm thick. Transistor is mounted asymmetrically at position 35mm from one edge as shown in Fig. 4.

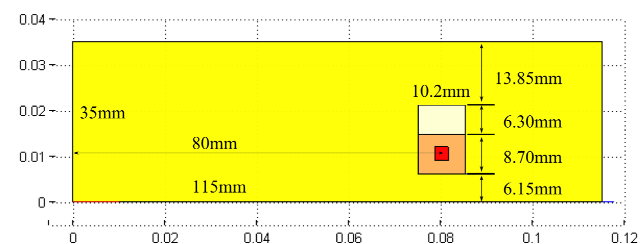

Fig. 4 Aluminium flat plate heat sink with dimensions 115mm long, 35mm wide, and 3mm thick. Transistor BDX53C in TO220 cases was mounted asymmetrically.

Copyright (c) 2013 International Journal of Computer Science Issues. All Rights Reserved.

Test circuit connects transistor as short-circuited constant current source. Collector-emitter voltage was V_{CE}=9.96V and emitter current was I_C=1.85A (neglecting dissipated power of base-emitter circuit), resulting in power dissipation of $P=V_{CE} \cdot I_C$=18.426W. Environment temperature was 31.43ºC, and no forced convection was used. Transistor was switched on at t=0s for duration of 90s. Heating phase was recorded with IR camera every 10s, and recording continued during cooling phase until 300s. Fig. 5 shows two measurements, first one is 50 seconds after transistor (heating) was switched on, and second one 210 seconds after transistor (heating) was switched off. Measurements were done with Fluke Ti25 IR camera [37]. Temperature of encircled part was recorded and plotted in Fig. 6(a), whereas simulation results with muphyPEEC are plotted in Fig. 6(b).

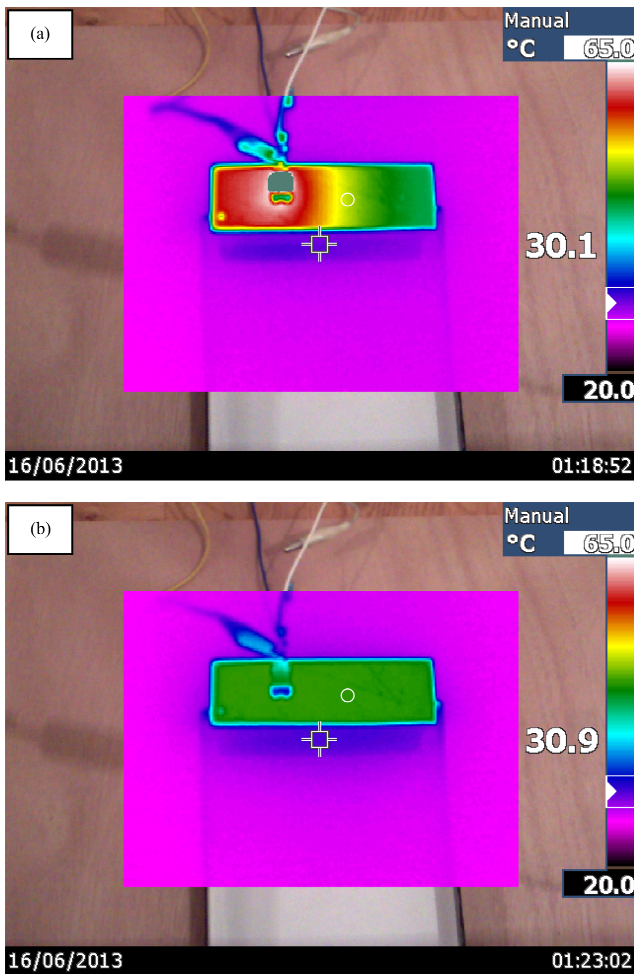

Fig. 5 IR camera recordings for flat plate heat sink with transistor BDX53C in TO220 cases: (a) Picture taken 50 seconds after transistor (heating) was switched on, gray color over transistor position signifies that temperature has excided maximum of selected range 65.0 [ºC], (b) Picture taken 210 seconds after transistor (heating) was switched off.

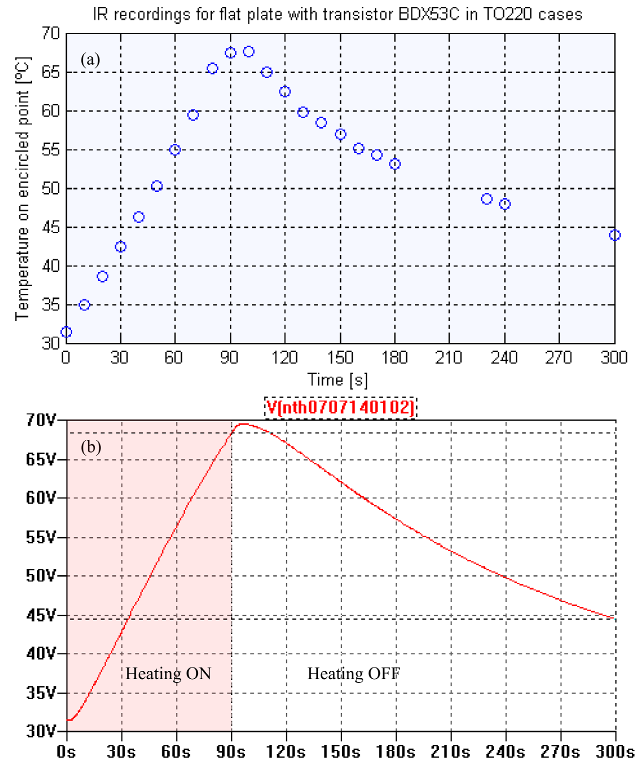

Fig. 6 Temperature of encircled point on flat plate heat sink: (a) Recordings from IR camera, (b) Simulation results with muphyPEEC.

To simulate the problem with muphyPEEC Toolbox as first step is to describe problem geometry according to wire-based language [16], [15]. Language has been extended with additional variables (global and local) and with instructions for defining boundary conditions. Defined geometry after meshing is shown in Fig. 7. Meshing for all domains is done with same function **GD2GDmesh** with requested resolution, which in general can be different for each domain. For this example only thermal meshing is requested, by setting global variables

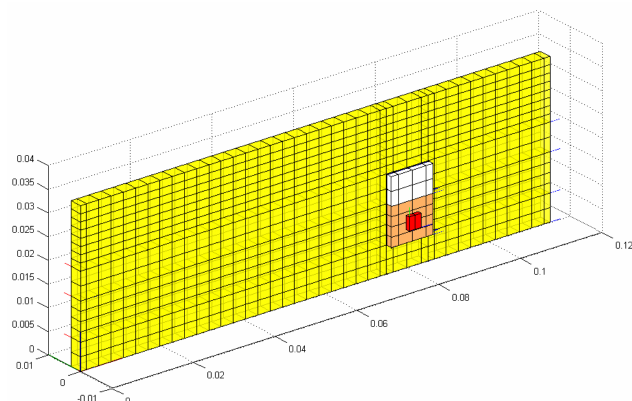

Fig. 7 Meshed geometry for flat plate with TO220 case.

Copyright (c) 2013 International Journal of Computer Science Issues. All Rights Reserved.

th_m=1 (default values is 0) for thermal meshing and el_m=0 (default value is 1) for disabling electromagnetic meshing. Calculation of partial elements and netlist generation with thermal PEEC model is done with function **GDmesh2Thermal**. Generated netlist will be included into LTspice, where simulation conditions and parameters will be defined, Fig. 8. It can be noticed usage of **.include** directive for inclusion of thermal PEEC netlist into LTspice environment. Thermal parameters are defined with **.params** directive. If simulation is to be done with known thermal (same holds for other domains) parameters, they can be given in *.gd file, and then there is no need for using parameter definition lines in LTspice. As a consequence, if some parameter needs to be changed, all steps will have to be repeated. Voltage source V2 sets the environment temperature Ta for natural convection, and V3 sets the thermal reference temperature N0th, zero in this case. I1 models heat generated at transistor junction. Since save LTspice directive was not used all circuit quantities (node voltages and branch currents) will be saved in *.raw file. This slows down simulation process and *.raw files can grow quite large. By adding save directive only listed quantities will be saved. Simulation lasted 37 seconds when "Alternate" solver was used, without save directive, and independent of integration method.

```
.params sal=0.9*205 cval=2.422*100*100*100
.params scu=401 cvcu=3.45*100*100*100
.params Ras=19 sisol=0.1*110 cvs=0.011

.params sB01=sal cvB01=cval
.params sB02=sal cvB02=cval
.params sB03=sal cvB03=cval
.params sB04=sal cvB04=cval
.params sB05=sal cvB05=cval
.params sB06=sal cvB06=cval
.params sB07=sal cvB07=cval
.params sB08=sal cvB08=cval
.params sB09=sal cvB09=cval
.params sB10=sal cvB10=cval
.params sB11=sal cvB11=cval
.params sB12=sal cvB12=cval

.params sB13=sisol cvB13=0.1*cval
.params sB14=sisol cvB14=0.1*cval

.params sB15=scu cvB15=cvcu
.params sB16=scu cvB16=cvcu

.params sB17=1/(0.25*2.08)*(0.001/2)/(0.003*0.003) cvB17=0.011/(0.003*0.003*0.001)

.include C:\PEEC_Toolbox\PEECspice_thermal_V01.00_LT.cir

Ta  N0th  Nth1717010101
V2  V3    I1
31.43  0  AC 1
PULSE(0 18.426 0 0.01 0.01 90)

.tran 0 300 0 0.1
```

Fig. 8 LTspice circuit for solving problem for flat plate and BDX53C transistor in TO220 case mounted on it.

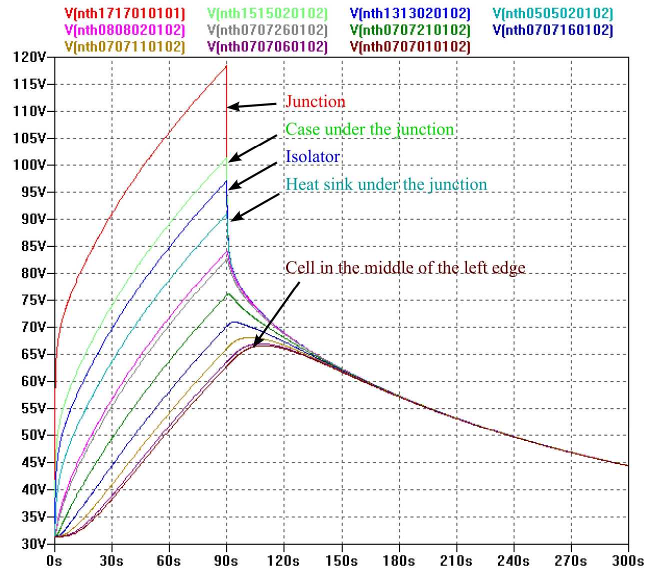

Fig. 9 Simulated temperature on different points of TO220 case and flat plate heat sink.

With save directive (5 node voltages were stored) simulation time went down to 22 seconds. Size of *.raw file was 15.9 MB (megabytes) in first case and 1.98 kB (kilobytes) in second. When "Normal" solver was used simulation lasted 27 seconds without save directive and 14 seconds with. Fig. 9 shows temperature from junction, through body and isolator, to heat sink cell under, then heat sink cell under the top of the TO220 fixing tab, and horizontally through encircled point till the edge of the heat sink.

6.2 Fin heat sink with transistor in TO220 case

Second example for testing muphyPEEC in thermal domain is transistor BDX53C in TO220 cases mounted on fin heat sink with natural convection shown in Fig. 10. Figure shows three projections of heat sink with dimensions: side view, top view, and front view. Two IR camera recordings are given in Fig. 11, where (a) photo is during heating phase and (b) photo is during cooling. Heating started at 21:01:00 (time marked on IR photos) and was stopped at 21:16:00. Recordings were done during 1500 seconds, with 900 seconds heating period. Transistor power dissipation was P=12.876W. Environment temperature was 27.8°C. Geometry was meshed for thermal domain only, Fig. 12. IR recorded temperature at measurement point during 1500 seconds, and simulation results can be seen in Fig. 13. From figure it can be seen that heating phase has very good match with measurements, but cooling in simulation is more intense than in measurements, caused by uniform convection coefficient over entire heat sink surface. For reference, simulation junction temperature was included in Fig. 13(b).

Copyright (c) 2013 International Journal of Computer Science Issues. All Rights Reserved.

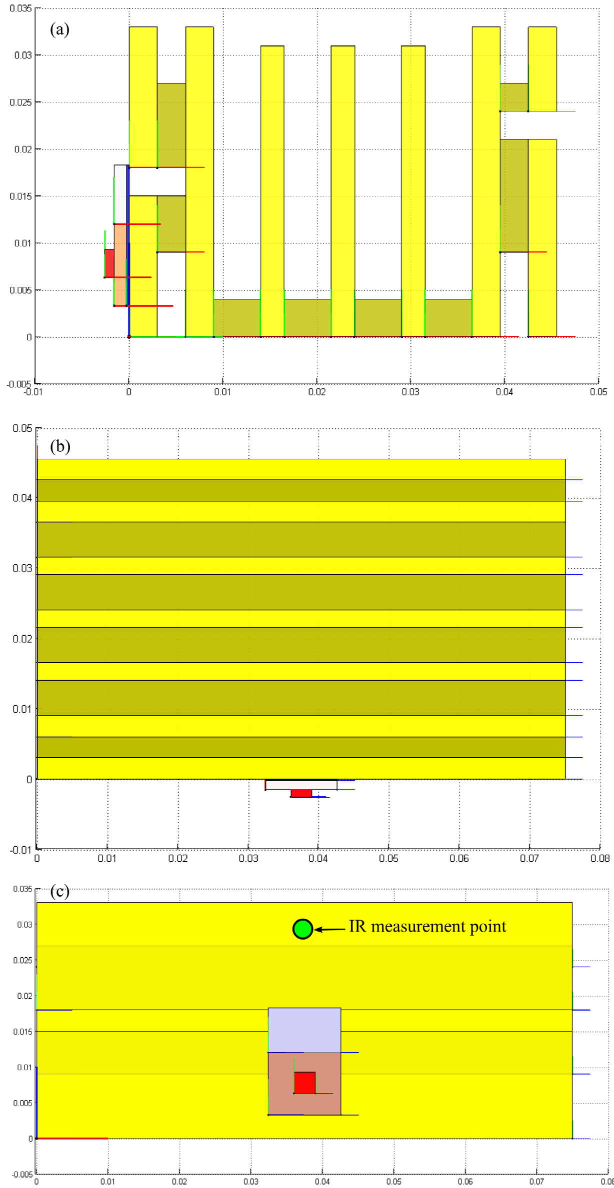

Fig. 10 Aluminium fin heat sink with transistor BDX53C in TO220 cases (a) Side view, (b) Top view, (c) Front view with circle marking the measure point for IR camera.

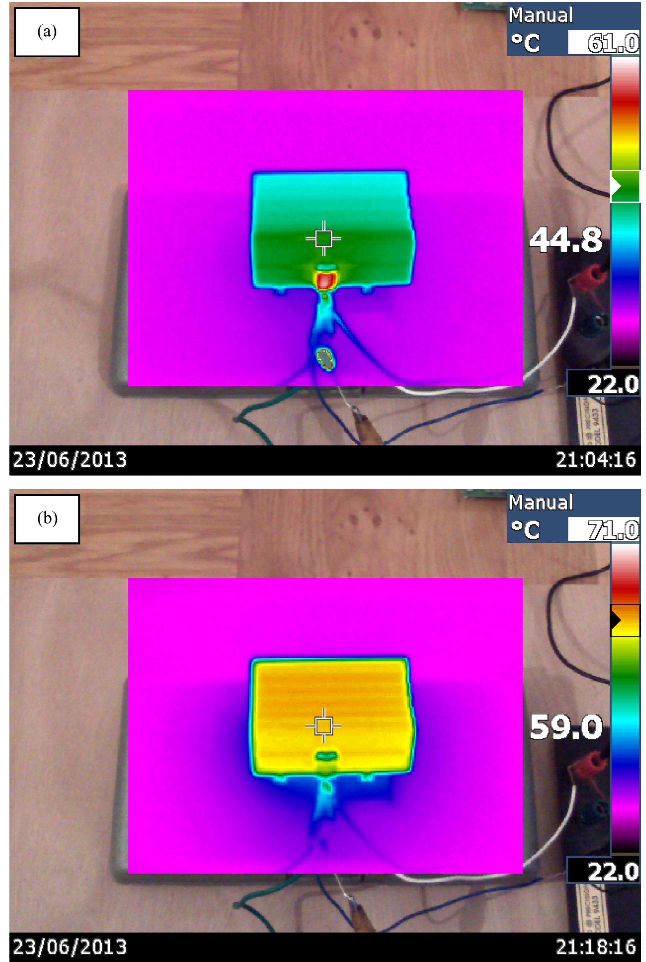

Fig. 11 IR camera recordings for fin heat sink with transistor BDX53C in TO220 cases: (a) Picture taken during heating phase, 570 seconds after heating started, (b) Picture taken during cooling phase, 135 seconds after heating was stopped.

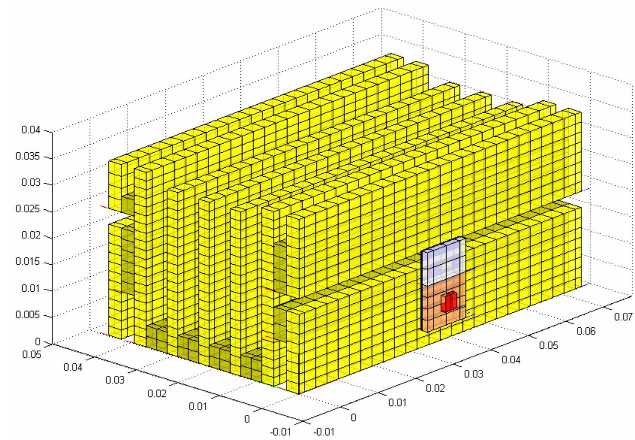

Fig. 12 Meshed geometry for fin heat sink with BDX53C transistor in TO220 cases.

Copyright (c) 2013 International Journal of Computer Science Issues. All Rights Reserved.

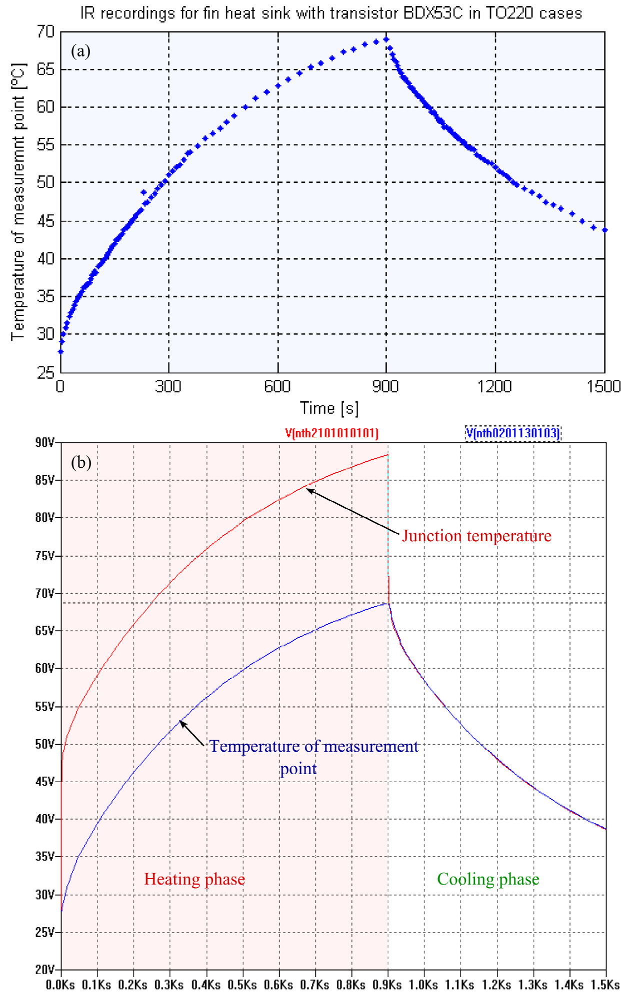

Fig. 13 Temperature of IR measurement point on fin heat sink: (a) Recordings from IR camera, (b) Simulation results with muphyPEEC.

6.3 Electro-thermal microactuator

Relative change in solid dimensions induced by temperature change is small, but with proper design and construction it can be used effectively for sensing and actuating [38], [39]. Thermal microactuators have advantage of generating high force with low voltages [40]. They can be constructed from two materials, like well known bimetalic constructions, or by using single material [41], [42]. Couplings between three domains are present in these actuators: electric, thermal, and mechanical. Approach used for analyzing single material (polysilicon) electro-thermal microactuators in [43] was fully coupled electro-thermal analyses, and after steady-state temperature field has been reached, elastic boundary value problem is solved. [17] used Matlab for thermal response and ANSYS [44] for structural response. Multiphysics approach was used in [45].

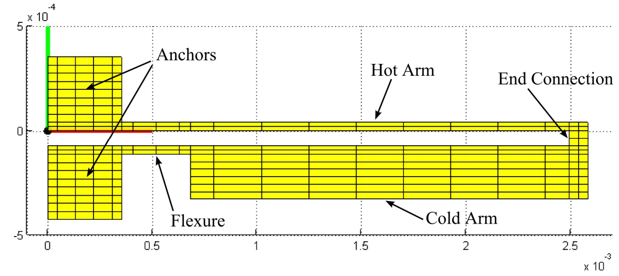

Fig. 14 Meshed Geometry for electro-thermal microactuator D2 from [43] in front view.

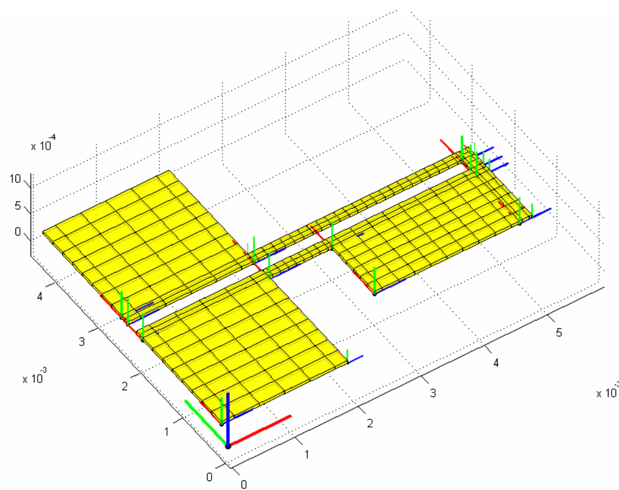

Fig. 15 Meshed Geometry for electro-thermal microactuator D3 from [43].

Simultaneous solution of three coupled electro-thermal-mechanical domains for electro-thermal microactuator (ETMA) D2 from [43] is used for third example for muphyPEEC. Same platform can be used for time- and frequency-domain response, so dynamic performance can be estimated [46]. Fig. 14 shows geometry of the ETMA D2, and Fig. 15 shows geometry of the ETMA D3 from [43]. Calculation of partial elements and netlist generation with thermal PEEC model is done with function **GDmesh2Thermal**, whereas for mechanical PEEC model it is done with function **GDmesh2Mechanical**. Three generated netlists are included into LTspice for simultaneous simulation. Thermal and mechanical circuit components are considered constant. Environment temperature is imposed as boundary condition at the device anchors. Convection heat transfer coefficients were considered constant for whole device. Radiation heat transfer has not been taken into account. Deflection of rightmost-top mechanical node of Hot-Arm in function of ETMA input voltage is shown in Fig. 16, for coefficient

Copyright (c) 2013 International Journal of Computer Science Issues. All Rights Reserved.

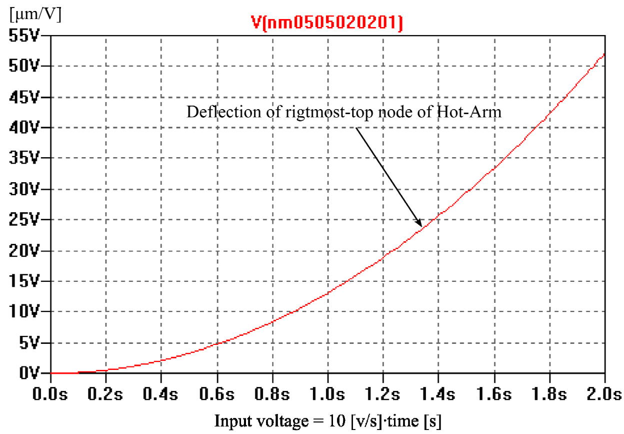

Fig. 16 Deflection of rightmost-top mechanical node (Nm0505020201) of Hot-Arm for electro-thermal microactuator D2 from [43] in function of input voltage from 0[V] to 20[V].

of thermal expansion α=4.099 [µm m^{-1} K^{-1}], thermal conductivity σ_{th}=40 [W m^{-1} K^{-1}], and convective heat transfer coefficient σ_c=80 [W m^{-2} K^{-1}]. Deflection at 19 [V] input was 47.2 [µm], as compared to around 40.5 [µm] in Fig. 5(a) of [43]. Table 1 summarizes this deflection as function of convective heat transfer coefficient.

Table 1: Electro-thermal microactuator deflection as function of convective heat transfer coefficient

Convective heat transfer coefficient σ_c [W m^{-2} K^{-1}]	***Deflection @19[V] [µm]***
0	48.56
10	48.70
20	48.79
30	48.84
40	**48.57**
50	48.30
60	47.98
70	47.60
80	47.20
90	46.77
100	46.32

It can be seen that deflection changes less than 5% for given range of values, but it has considerable influence in arms working temperature and limit for highest operating voltage. Table 2 summarizes ETMA deflection as function of material thermal conductivity for range of values given in Table 5 of [43], and considerable influence is noticeable, from around 71.7 [µm] to 13.0 [µm]. Wide range of variability on these parameters suggests that they

Table 2: Electro-thermal microactuator deflection as function of material thermal conductivity

Material thermal conductivity σ_t [W m^{-1} K^{-1}]	***Deflection @19[V] [µm]***
25.1	71.66
26.1	69.30
27.2	68.86
28.2	64.79
31.4	58.91
34.5	54.10
37.6	49.99
40.0	**47.20**
41.8	45.29
49.2	38.79
57.5	33.35
73.2	26.28
98.3	19.53
146.4	13.02

can not be treated as constants, and temperature dependence for these parameters has to be implemented.

Frequency response of the structure is given in Fig. 17. Since problem is nonlinear, frequency response is

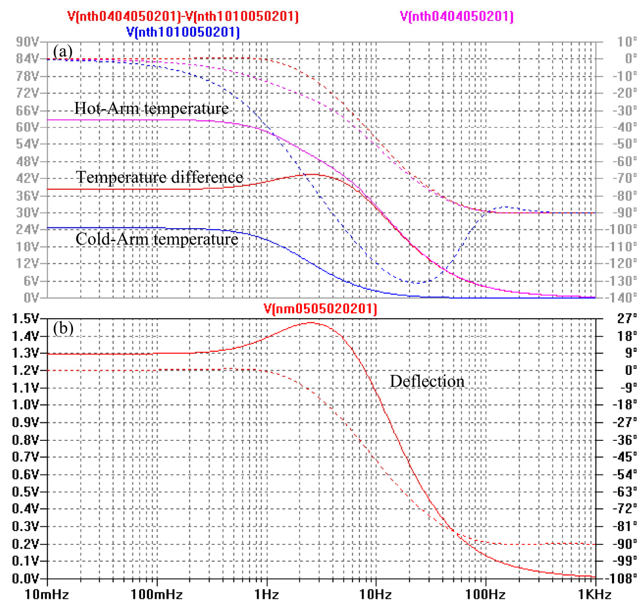

Fig. 17 Frequency response of electro-thermal microactuator at 5 [V] operating point under 1 [V] sinusoidal excitation: (a) Frequency response for the Hot-Arm temperature, the Cold-Arm temperature, and for the temperature difference, with Volt unit equivalent to ºC. (b) Frequency response for deflection, with Volt unit equivalent to µm.

Copyright (c) 2013 International Journal of Computer Science Issues. All Rights Reserved.

dependent on selected operation point and on amplitude of sinusoidal excitation. Response in figure is at 5 [V] operation point and 1 [V] for amplitude of excitation. To record frequency response of PEEC model, first parameter is given as "DC offset" of sinusoidal source, and second parameters is given as "AC amplitude".

7. Conclusions

Extension of Partial Element Equivalent Circuit (PEEC) method with possibility of solving other physical domains has been presented. Extension is generally based in circuit interpretation of Finite Difference (FD) or Finite Element Method (FEM) equations. For one multiphysics cell PEEC building block will be composed from as many single domain building block as accounted physical domains, plus couplings between some or all single domain blocks. Couplings are through components or sources of one domain block dependent on variables of other domain block. Dependence can be also from the same physical domain variables, leading to single domain nonlinear PEEC models. Discretization for each domain can be different. In this case one block from one domain may be dependent from many blocks from other domain and vice versa. All steps from geometry description to netlist generation for all domains are done in MATLAB with muphyPEEC Toolbox. Solution of the problem in time- or frequency-domain is done with LTspice. Thermal (with no radiative heat transfer) and mechanical domains generate system matrixes that are block diagonal and sparse, contrary to fully coupled electromagnetic domain, and they can be solved very efficiently with Spice solvers, since they are optimized specifically for solving sparse systems. Efficiency of muphyPEEC to solve coupled electro-thermal problems is demonstrated with examples and results are compared with IR (Infra Red) camera recordings. Cooling phase of fin heat sink suggests that with complex geometries convection heat transfer needs more detailed treatment. When couplings between domains are in limited space, it would be possible to approximate problem with decoupled blocks, leading to system level simulations. Fully coupled simulations of electro-thermal microactuator could predict deflection in function of input voltage, but it shows high sensitivity to variability of material thermal properties from temperature, and for accurate behavior prediction they must be accounted for. Spice family of circuit solvers offer frequency-domain analysis as standard simulation mode, but when it is used to nonlinear systems, like electro-thermal microactuator, results will depend on operation point (that must be properly set up), and also on the amplitude of excitation signal.

References

[1] James W. Nilsson, Susan A. Riedel, Electric Circuits, 6th Edition, Prentice-Hall, Inc., 2001.

[2] L. W. Nagel and D. O. Pederson, “SPICE (Simulation Program with Integrated Circuit Emphasis), “Memorandum No. ERL-M382, University of California, Berkeley, Apr. 1973.

[3] Laurence W. Nagel., “SPICE2: A Computer Program to Simulate Semiconductor Circuits”, Memorandum No. ERL-M520, University of California, Berkeley, May 1975.

[4] Andrei Vladimirescu, The Spice Book, John Wiley &Sons, Inc., 1994.

[5] Farid N. Najm, Circuit Simulation, John Wiley &Sons, Inc., 2010.

[6] Linear Technology, LTspice IV. http://www.linear.com/designtools/software/#LTspice

[7] Tadej Tuma, Árpád Bürmen, Circuit Simulation with SPICE OPUS: Theory and Practice, Birkhäuser, 2009.

[8] Harry F. Olson, Dynamical Analogies, D. van Nostrand Company, Inc., 1943.

[9] Brian C. Fabian, Analytical System Dynamics: Modeling and Simulation, Springer Science+Business Media, LLC 2009

[10] John J. D'Azzo, Constantine H. Houpis, Linear Control System Analysis and Design: Conventional and Modern, 3rd Edition, McGraw-Hill, Inc., 1988.

[11] Yuling Shang, Chunquan Li, Huaqing Xiong, "One Method for Via Equivalent Circuit Extraction Based on Structural Segmentation", IJCSI International Journal of Computer Science Issues, Vol. 10, Issue 3, No 1, May 2013.

[12] Albert E. Ruehli, "Equivalent Circuit Models for Three-Dimensional Multiconductor Systems", IEEE Trans. on Microwave Theory and Techniques, Vol. MTT-22, No.3, March 1974.

[13] J. Nitsch, F. Gronwald, G. Wollenberg, Radiating Non-Uniform Transmis-sion Line Systems and the Partial Element Equivalent Circuit Method, John Wiley & Sons, Ltd, 2009.

[14] D. Gope, A. Ruehli, and V. Jandhyala, "Solving low-frequency EM-CKT problems using PEEC method", IEEE Trans. on Advanced Packaging, col. 30, no. 2, May 2007

[15] Vjosa Shatri, Ruzhdi Sefa, and Lavdim Kurtaj, "MATLAB Partial Element Equivalent Circuit Toolbox for Solving Coupled Electromagnetic-Circuit Problems", International Journal of Current Engineering and Technology, Vol.3, No.4, 2013.

[16] Vjosa Shatri, Ruzhdi Sefa, Lavdim Kurtaj, "Partial Element Equivalent Circuit (PEEC) Toolbox for MATLAB, integrating FastCap2 and FastHenry2 to Calculate Partial Elements, and Multisim or LTspice for circuit simulation", Proceedings of the 12th WSEAS International Conference on Systems Theory and Scientific Computation (ISTASC '12), Istanbul, Turkey, August 21-23, 2012.

[17] M. S. Baker, R. A. Plass, T. J. Headley, & J. A. Walraven, "Compliant Thermomechanical MEMS Actuators", Final Report, Sandia National Laboratories, Albuquerque, NM, 2004.

[18] Enrico Vialardi, Edith Clavel, Olivier Chadebec, Jean-Michel Guichon and Marie Lionet, "Electromagnetic Simulation of Power Modules via Adapted Modelling Tools", EPE-PEMC 2010 14th International Power Electronics and Motion Control Conference, 2010.

Copyright (c) 2013 International Journal of Computer Science Issues. All Rights Reserved.

[19] Massimiliano Margonari, "A simple finite element solver for thermo-mechanical problems", Enginsoft S.p.A., 2010.

[20] Petr Krysl, A Pragmatic Introduction to the Finite Element Method for Thermal and Stress Analysis: With the Matlab toolbox SOFEA, Pressure Cooker Press, November 2005.

[21] Thomas J. R. Hughes, The Finite Element Method: Linear Static and Dynamic Finite Element Analysis, Prentice-Hall, Inc., 1987.

[22] Matthew N. O. Sadiku, Numerical Techniques in Electromagnetics, CRC Press, 2001.

[23] R.W. Lewis, P. Nithiarasu and K. N. Seetharamu, Fundamentals of the Finite Element Method for Heat and Fluid Flow, Wiley Ltd., 2004.

[24] Pavel V. Nikitin, Erik Normark, and C.-J. Richard Shi, "Distributed Electrothermal Modeling in VHDL-AMS", Behavioral Modeling and Simulation, 2003. BMAS 2003. Proceedings of the 2003 International Workshop on, 7-8 Oct. 2003.

[25] Rhythm-Suren Wadhwa, "Electromagnet Gripping in Iron Foundry Automation Part II: Simulation", IJCSI International Journal of Computer Science Issues, Vol. 9, Issue 2, No 2, March 2012.

[26] Anis Ammous, Sami Ghedira, Bruno Allard, Herve' Morel, and Denise Renault, "Choosing a Thermal Model for Electrothermal Simulation of Power Semiconductor Devices", IEEE Trans. on Power Electronics, Vol. 14, No. 2, March 1999.

[27] U. Drofenik, A. Müsing, and J. W. Kolar, "Voltage-Dependent Capacitors in Power Electronic Multi-Domain Simulations", Power Electronics Conference (IPEC), 2010.

[28] U. Drofenik, D. Cottet, A. Müsing, J. W. Kolar, "Design Tools for Power Electronics: Trends and Innovations", Proceedings of the 2nd International Conference on Automotive Power Electronics (APE '07), 2008.

[29] Daryl L. Logan, A First Course in the Finite Element Method, Fourth Edition, Nelson, a division of Thomson Canada Limited, 2007.

[30] Jia Tzer Hsu and Loc Vu-Quoc, "A Rational Formulation of Thermal Circuit Models for Electrothermal Simulation: I. Finite Element Method", Circuits and Systems I: Fundamental Theory and Applications, IEEE Transactions on, Vol. 43, Issue 9, Sep 1996, pp. 721-732.

[31] C. Bohm, T. Hauck, E. B. Rudnyi, J. G. Korvik, "Compact Electro-thermal Models of Semiconductor Devices with Multiple Heat Sources", Thermal and Mechanical Simulation and Experiments in Microelectronics and Microsystems, EuroSimE 2004. Proceedings of the 5th International Conference on, 2004, pp. 101-104.

[32] Vjosa Shatri, Ruzhdi Sefa, Lavdim Kurtaj, "Relative Position between Mesh Cell Edges and Interrelation with Accuracy when using FastCap2 for Capacitance Calculations of 3-D PEEC-like Cells", Proceedings of the 12th WSEAS International Conference on Systems Theory and Scientific Computation (ISTASC '12), August 21-23, 2012, pp. 213-218.

[33] Sinigiresu S. Rao, The Finite Element Method in Engineering, Fifth Edition, Elsevier, 2011.

[34] J. P. Holman, Heat Transfer, Tenth Edition, McGraw-Hill Companies, Inc., 2010.

[35] Scott Pearson, Alain Laprade, "Tips and Tricks to Get More Out of Your SPICE Models", Fairchild Power Seminar 2007.

[36] Dalibor Biolek, Zdenek Kolka, Viera Biolkova, "Modeling time-varying storage components in PSpice", Proceedings of the Electronic Devices and Systems IMAPS CS International Conference EDS 2007, 2007, pp. 39-44.

[37] Fluke, "Ti9, Ti10, Ti25, TiRx, TiR and TiR1 Thermal Imagers", Users Manual, Fluke Corporation, 2010.

[38] Yukun Jia and Qingsong Xu, MEMS "Microgripper Actuators and Sensors: The State-of-the-Art Survey", Recent Patents on Mechanical Engineering, Vol. 6, 2013.

[39] Ki Bang Lee, Principles of Microelectromechanical Systems, John Wiley & Sons, Inc., 2011.

[40] Leslie M. Phinney, Michael S. Baker and Justin R. Serrano, "Thermal Microactuators", in Microelectromechanical Systems and Devices, Edited by Nazmul Islam, InTech, March 28, 2012, pp. 415-434.

[41] Qing-An Huang and Neville Ka Shek Lee, "Analysis and design of polysilicon thermal flexure actuator", J. Micromech. Microeng., Vol. 9, 1999, pp. 64–70.

[42] Amarendra Atre and Stephen Boedo, "Effect of Thermophysical Property Variations on Surface Micromachined Polysilicon Beam Flexure Actuators", NSTI-Nanotech 2004.

[43] Nilesh D Mankame and G K Ananthasuresh, "Comprehensive thermal modelling and characterization of an electro-thermal-compliant microactuator", J. Micromech. Microeng., Vol. 11, 2001, pp. 452–462.

[44] Y. Nakasone, T. A. Stolarski and S. Yoshimoto, Engineering Analysis with ANSYS Software, Elsevier Butterworth-Heinemann, 2006.

[45] Tanu Pahwa,Shefali Gupta, Vineet Bansal, B.Prasad, Dinesh Kumar, "Analysis & Design Optimization of laterally driven Poly-Silicon Electro-thermal Micro-gripper for Micro-objects Manipulation", Proceedings of the 2012 COMSOL Conference in Bangalore, 2012.

[46] Chih-Ching Lo, Meng-Ju Lin, and Chung-Li Hwan, "Modeling and Analysis of Electro-Thermal Microactuators", Journal of the Chinese Institute of Engineers, Vol. 32, No. 3, 2009, pp. 351-360.

Copyright (c) 2013 International Journal of Computer Science Issues. All Rights Reserved.